Original Article

Iron Overload Causes Alterations of E-Cadherin in the Liver

(iron overload / E-cadherin / liver / adherens junctions)

Y. FUJIKURA[1, 3], J. KRIJT[1], C. POVÝŠIL[2], Z. MĚLKOVÁ[3], P. PŘIKRYL[1], M. VOKURKA[1], E. NEČAS[1]

[1]Institute of Pathophysiology, [2]Institute of Pathology, [3]Institute of Immunology and Microbiology, First Faculty of Medicine, Charles University in Prague, Czech Republic

Abstract. Iron overload causes tissue damage in the liver, but its initial effects at the molecular and cellular level are not well understood. Epithelial cadherin (E-cad) is a major adhesion protein in adherens junctions and is associated with several signal transduction pathways. Dysfunction of E-cad causes instability of adherens junctions, which leads to cell invasion, cell migration, and carcinogenesis. We found in liver samples from iron-overloaded mice that the apparent molecular mass of E-cad was reduced from 125 to 115 kDa in sodium dodecyl sulphate polyacrylamide gel electrophoresis under reducing conditions and immunoblotting, and that the cellular expression of E-cad was decreased in immunohistochemistry. The mRNA level of E-cad, however, did not change significantly, suggesting that the alterations are posttranslational. Interestingly, incubation of control liver extracts with Fe^{2+} alone also produced the same mobility shift. Neither an oxidant nor an antioxidant influenced this shift *in vitro*, suggesting that reactive oxygen species, which are generated by iron and known to cause damage to macromolecules, are not involved. Treatment of the 115 kDa E-cad with deferoxamine, an iron chelator, thus removing Fe^{2+}, shifted the molecular mass back to 125 kDa, demonstrating that the shift is reversible. The observation also implies that the alteration that causes the mobility shift is not due to transcriptional control, deglycosylation, and proteolysis. This reversible mobility shift of E-cad has not been previously known. The alteration of E-cad that causes the mobility shift might be an initial step to liver diseases by iron overload.

Received June 25, 2015. Accepted March 23, 2016.

This work was supported by the grants PRVOUKP24/LF1/3 and SVV 2014-260033 from Charles University in Prague, Czech Republic.

Corresponding author: Yuzo Fujikura, Institute of Immunology and Microbiology, First Faculty of Medicine, Charles University in Prague, Studničkova 7, 12800 Prague 2, Czech Republic Phone: (+420) 224 968 460; Fax: (+420) 224 968 588; e-mail: yuzofujikura@hotmail.com

Abbreviations: AJs – adherens junctions, DFO – deferoxamine, E-cad – epithelial cadherin, *Hjv*$^{+/+}$ – haemojuvelin wild type, *Hjv*$^{-/-}$ – haemojuvelin knock out, LB – lysis buffer, ROS – reactive oxygen species.

Introduction

Primary iron overload is a genetic disorder of iron metabolism causing inappropriately increased iron absorption due to a defect in the hepcidin signalling pathway as seen in hereditary haemochromatosis; secondary (acquired) iron overload most often develops as a complication of repeated transfusions and is associated with cardiomyopathy and chronic liver diseases (Pietrangelo, 2003; Sebastiani and Pantopoulos, 2011). Iron itself is not carcinogenic. However, iron overload is associated with tissue damage and carcinogenesis. Primarily iron overload causes fibrosis, most frequently in the liver, heart, and pancreas. The liver fibrosis due to iron excess evolves into cirrhosis and may eventually lead to the development of hepatocellular carcinoma. In pathological iron overload, iron gradually saturates the iron-binding capacity of transferrin, which under physiological conditions maintains iron soluble and nontoxic (Ponka et al., 1998), and non-transferrin-bound iron eventually gets internalized into cells. Iron's toxicity is largely based on its ability to generate reactive oxygen species (ROS) (Halliwell and Gutteridge, 1990), an increase of which beyond the antioxidant capacity of the organism causes oxidative stress (Papanikolaou and Pantopoulos, 2005). Although iron-induced chronic oxidative stress is known to cause damage to macromolecules, the mechanisms of initial tissue damage triggered by iron overload are not well understood.

Cell adhesion proteins cadherins are single-pass transmembrane glycoproteins that are built on the contacts between adjacent cells. Extracellular domains of cadherins on the opposing membranes mediate Ca^{2+}-dependent homophilic interaction and cytoplasmic domains form a complex with catenins (α-, β-, γ-, and p120), which interact with actin filaments and microtubules (Meng and Takeichi, 2009). In this way cadherins, together with

several adaptor proteins, functionally link the cytoskeleton of adjacent cells (Taguchi et al., 2011) and contribute to cell-cell adhesion to form mature adherens junctions (AJs). E-cad is the major cadherin in liver epithelial cells and is directly bound by β- and p120 catenin. The binding of the catenins masks sequences containing the motif of the E-cad degradation pathway (Huber et al., 2001; Miyashita and Ozawa, 2007; Nanes et al., 2012). Some of cell surface E-cad is constitutively endocytosed to regulate cadherin-based adhesion, through which E-cad is degraded by lysosome and/or proteasome, or recycled back to the plasma membrane (Le et al., 1999; Davis et al., 2003; Xiao et al., 2003).

Inactivation of the E-cad cell adhesion system causes organ fibrosis due to the reduced cell-cell adhesiveness (Hirohashi, 1998; Guarino et al., 2009). A correlation between the cellular expression of the E-cadherin/catenin complex and the development and progression of hepatocellular carcinoma has been reported (Zhai et al., 2008). E-cad-mediated cell adhesion is known to be inactivated by genetic alterations and transcriptional repression (Berx et al., 1998; Alves et al., 2009). However, it has been suggested that E-cad dysfunction cannot be explained at the genetic/epigenetic level alone and that other mechanisms may operate at the posttranslational level (Pinho et al., 2011) in response to changes in external/internal signals.

While investigating membrane proteins in the liver, we noticed that the intensity and mobility of cadherin bands were altered when the iron content of samples was high. Since the direct effect of iron on E-cad in the liver has not been fully elucidated, we investigated E-cad in the liver from iron-overloaded mice, in order to detect possible initial alterations of E-cad by iron overload. Liver samples were analysed at the molecular and cellular level by immunoblotting and immunohistochemistry, respectively. The detected alterations may provide better understanding of the initiation of liver diseases by iron overload.

Material and Methods

Animals

Haemojuvelin wild type (*Hjv*$^{+/+}$) and knock out (*Hjv*$^{-/-}$, a model of juvenile haemochromatosis) mice were a generous gift from Prof. Silvia Arber, Basel, Switzerland (Niederkofler et al., 2005). Iron-overloaded mice of the C57BL/6 strain were prepared by injection of iron dextran (Sigma-Aldrich, St Louis, MO) at 200 mg iron/kg, and after three days liver samples were obtained. All animal experiments were approved by the Ethics Committee of the First Faculty of Medicine, Charles University in Prague.

Protein extraction

Liver protein was extracted in lysis buffer (LB) described by Reynolds et al. (1994): 20 mM Tris-HCl pH 7.4 containing 0.5% NP-40, 150 mM NaCl, 1 mM EDTA, Protease Inhibitor Cocktail (Roche, Basel, Switzerland), and Phosphatase Inhibitor Cocktails 2 and 3 (Sigma-Aldrich). Extracts were obtained by homogenizing 20–50 mg of tissue in 250 µl of LB and subsequent centrifugation at 14,000 *g* for 15 min at 4 °C. For fractionation, protein was extracted in 20 mM Tris-HCl pH 6.8 containing 0.28 M sucrose, 50 mM NaCl, 2 mM EDTA, and the protease and phosphatase inhibitor cocktails. The homogenate was centrifuged at 6,000 *g* for 15 min to remove large membrane fragments (P1), and the supernatant was centrifuged at 16,000 *g* for 45 min. The pellet that contains membrane proteins was saved (P2) and the supernatant was subjected to ultracentrifugation at 80,000 *g* for 55 min. The pellet that contains endosomes (Hoshino et al., 2005) was saved (P3). P2 and P3 were washed once and dissolved in LB. For the dose response tests, LB extracts of the liver from C57BL/6 mice subjected to different doses of iron, 200, 350, and 700 mg/kg, were prepared. Protein concentration was measured by Bradford reagent (Sigma-Aldrich) with BSA as the standard. Other chemicals were obtained from Sigma-Aldrich.

Immunoblotting

Proteins, 50 or 60 µg of each sample, were separated in 6 or 8% SDS-PAGE under reducing conditions and transferred to PVDF membrane (GE Healthcare, Little Chalfont, UK) by electroblotting. The standard procedure using TBS containing 0.1% Tween-20 (TBS/T) for washing, 5% (w/v) non-fat milk in TBS/T for blocking, 16 h incubation at 4 °C with the rabbit primary antibody (E-cad: 1 : 3000, Cell Signaling Technology, #3195, Danvers, MA; actin: 1 : 8000, Sigma-Aldrich) in TBS/T and 2 h incubation at room temperature with the peroxidase-conjugated anti-rabbit secondary antibody (1 : 1000, Jackson Immuno Research, West Grove, PA) in TBS/T was employed. Positive signals were detected by the chemiluminescence method (Cell Signaling Technology). BenchMark Protein Ladder (Invitrogen, Carlsbad, CA) was used to estimate the molecular mass of protein bands. The immunoblots are representatives of at least two independent experiments.

mRNA measurement

Liver RNA was isolated using a Qiagen RNeasy Plus Mini Kit (Qiagen GmbH, Stockach, Germany). cDNA was synthesized using a Fermentas RevertAid First Strand cDNA Synthesis Kit (Thermo Fisher Scientific, Waltham, MA). For real-time PCR determination of E-cad gene (*Cdh1*) expression, a Roche LightCycler instrument in combination with the Fast Start SYBR Green protocol (Roche Diagnostics GmBH, Mannheim, Germany) was used. Target mRNA content was calculated relative to GAPDH mRNA content. Primers (forward and reverse) were as follows: *Gapdh*, CGGTGTGAACGGATTTGC and GCAGTGATGGCATGGACTGT, and *Cdh1*, CCATGTGTGTGACTGTGAAGG and CAGCTGGCTCAAATCAA AGTC.

Fe^{2+} in vitro assays

Extracts containing 50 μg of protein in LB were subjected to the treatment in 50 μM Hepes pH 7.5 containing 100 mM NaCl, 2 mM DTT, and the protease inhibitor cocktail at the final volume of 20 μl. For detection of the effects of Fe^{2+}, extracts were incubated with $FeSO_4$ at 1 mM for 30 min at 30 °C. For the dose response check, control extracts were treated with different concentrations of $FeSO_4$. For H_2O_2 assay, control extracts were incubated with different concentrations of H_2O_2 for 30 min at 30 °C. For N-acetylcysteine, glutathione, and dithiothreitol assays, control extracts were first incubated with the agent for 5 min, and then $FeSO_4$ was added at 1 mM, followed by 30 min incubation at 30 °C. Deferoxamine (DFO) was added to the extracts after 30 min incubation with $FeSO_4$ at 1 mM at 30 °C, and the extracts were further incubated for 30 min. Extracts from C57BL/6 iron-overload mice generated by injection of iron dextran (700 mg/kg body weight) were also tested for the DFO treatment. Since phosphorylation may be involved in the shift, LB extracts that contained phosphatase inhibitors were diluted more than ten times in the assays so that the influence of the inhibitors was negligible. All the reagents were obtained from Sigma-Aldrich.

Immunohistochemistry

Liver samples were fixed in formalin and embedded in paraffin, from which histological sections were collected. For protein detection, sections were dewaxed and incubated with methanol containing 30% H_2O_2 for 20 min to block endogenous peroxidase activity. Sections were then immersed in 10 mM citrate buffer pH 6.0 and heated in a microwave oven at 100 °C for 20 min to enhance antigen retrieval, washed three times with distilled water, and blocked with 1% BSA for 30 min. Subsequently, sections were incubated overnight at 4 °C with antibody, first with anti E-cad (1 : 400, Cell Signaling and Technology), then with the peroxidase-conjugated secondary antibody (1 : 500, Jackson Immuno Research) for 30 min at 37 °C. Finally, sections were washed three times with PBS buffer and the colour was displayed with DAB. Nuclei were lightly counterstained with haematoxylin. Perl's iron stain method was used for detection of iron deposition.

Results

Mobility shift of E-cadherin in the liver of iron-overloaded mice

First, we compared the livers from *Hjv*$^{+/+}$ mice (liver iron content less than 100 μg/g wet weight) with those from *Hjv*$^{-/-}$ mice (liver iron content approximately 2000 μg/g wet weight), a murine model of juvenile haemochromatosis (Niederkofler et al., 2005). Liver extracts were prepared in LB and analysed by immunoblotting. In the control sample, the E-cad band was detected at around 125 kDa in our system, whereas in the iron overload sample, in addition to a less intense 125 kDa band, an extra band was also detected approximately at 115 kDa (Fig. 1A), clearly demonstrating that iron overload caused an alteration of E-cad expression, which was detected as a reduction of the apparent molecular mass, a mobility shift. Detection of the two E-cad bands in the iron overload sample by E-cad antibody from a different manufacturer confirmed the observation (data not shown).

Second, in order to check the *Hjv*$^{-/-}$-specificity of the mobility shift, the livers from *Hjv*$^{+/+}$ and *Hjv*$^{-/-}$ mice were compared with those from control C57BL/6 (C, liver iron content 70 μg/g wet weight) and iron dextran-treated C57BL/6 (Fe, liver iron content approximately 1400 μg/g wet weight) mice. To also detect possible cellular localization of the 115 kDa E-cad at the same time, liver samples from the two strains were homogenized in detergent-free buffer and subjected to differential centrifugation. In control samples from both strains, E-cad was detected only as the 125 kDa band (Fig. 1B. 1, 3, 5, 7), whereas the 115 kDa band was detected in iron overload samples from both strains (Fig. 1B. 2, 4, 6, 8), indicating that the shift is not strain-specific. The P2 fraction contains membrane proteins and the P3 fraction contains endosomes (Hoshino et al., 2005). Whereas in the P2 fraction, Hjv and C57BL/6 samples showed a similar pattern (Fig. 1B. 1, 2, 5, 6), in the P3 fraction, only a faint 115 kDa band was detected for *Hjv*$^{-/-}$, while the two bands were detected for Fe (Fig. 1B, 4, 8). The result suggested a dose dependency of the mobility shift since the iron content of Fe is much lower than that of *Hjv*$^{-/-}$; the dose response of the alteration *in vivo* was tested by increasing amounts of iron dextran injected into C57BL/6 mice and samples extracted in LB indeed revealed the dose dependency (Fig. 1C). Since the P2 fraction contained much more protein than the P3 fraction, the majority of the 115 kDa E-cad was observed in the P2 fraction. Meanwhile, only an insignificant difference in the E-cad mRNA level was detected between *Hjv*$^{+/+}$and *Hjv*$^{-/-}$, as well as between C57BL/6 control (C) and iron-injected samples (Fe) (Fig. 1D).

Mobility shift of E-cadherin by Fe^{2+} in vitro

Interestingly, when the control extract from C57BL/6 mice, which contained only 125 kDa E-cad, was incubated with $FeSO_4$ at 1 mM, the mobility shift to 115 kDa was observed (Fig. 2A. 1, 3). The same shift occurred for the 125 kDa E-cad in the iron overload sample, but no further change was observed for the 115 kDa band (Fig. 2A. 2, 4). The size of the shifted E-cad band for both samples appeared the same at 115 kDa. The shift *in vitro* was also found to be dose-dependent (Fig. 2B).

Effect of oxidative stress on the mobility shift of E-cad

Excess levels of ROS generated by iron cause oxidative stress, which results in damage to proteins. We

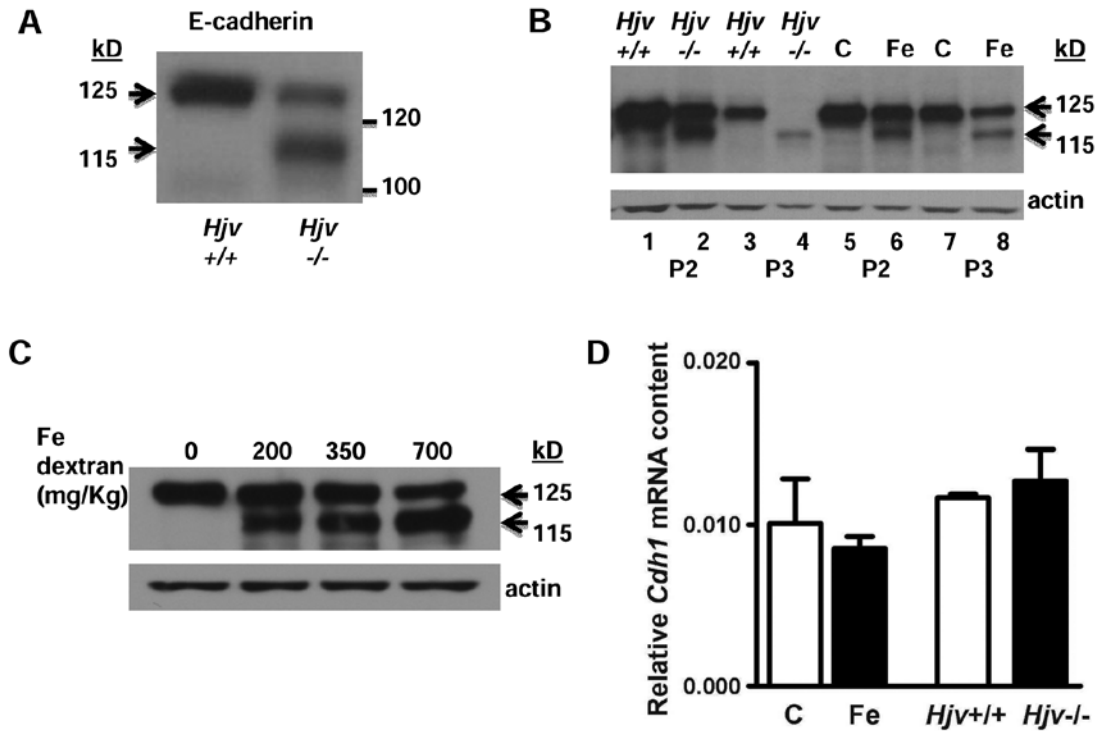

Fig. 1. Effects of iron overload on E-cadherin in the liver. (**A**) Immunoblot of E-cad extracted in LB. *Hjv*$^{+/+}$, control; *Hjv*$^{-/-}$, iron overload by haemojuvelin gene disruption, a mouse model of juvenile haemochromatosis. Arrows indicate E-cad bands. Bars indicate the location of the molecular weight standard. (**B**) E-cad extracted in detergent-free buffer and fractionated by differential centrifugation. C, C57BL/6 control; Fe, C57BL/6 iron overload by injection of iron dextran; P2, pellet of the second centrifugation, containing membrane-bound proteins; P3, pellet of the third/ultra centrifugation, containing endosomes. (**C**) Iron dose response of the mobility shift of E-cad *in vivo*. Different doses of iron dextran (mg/kg body weight) were examined. (**D**) E-cad (Cdh1) expression detected by real-time PCR. Error bars represent the standard deviation of three experiments.

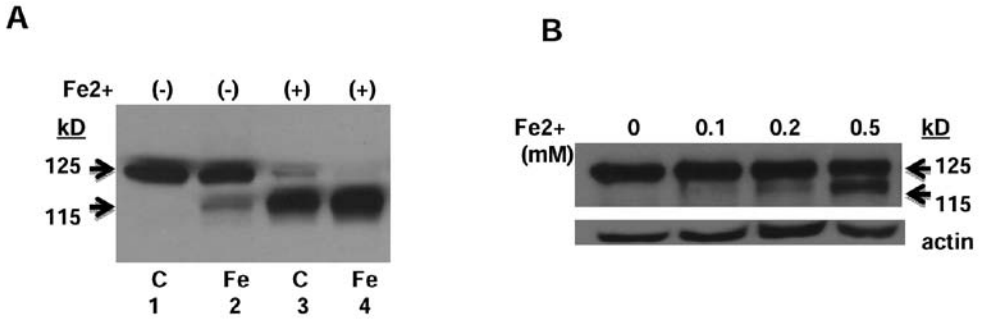

Fig. 2. Effect of Fe^{2+} on E-cadherin *in vitro*. (**A**) Immunoblot of E-cad in LB extracts incubated with $FeSO_4$ at 1 mM for 30 min at 30 °C. C, C57BL/6 control; Fe, C57BL/6 iron overload by injection of iron dextran; Fe2+, $FeSO_4$. (**B**) Iron dose response of the mobility shift of E-cad. Control extracts were incubated with $FeSO_4$ at different concentrations.

therefore examined the influence of ROS on the mobility shift of E-cad. Extracts were subjected to treatment with either an oxidant or an antioxidant. When the control extracts from C57BL/6 mice were incubated with a wide range of concentrations of the oxidant H_2O_2, 2–50 mM, no mobility shift of E-cad was detected (Fig. 3A). N-acetylcysteine has been used as a therapeutic agent against oxidation. Pre-incubation with N-acetylcysteine at up to 1 mM did not affect the shift caused by subsequent treatment with $FeSO_4$ at 1 mM (Fig. 3B). Glutathione is a critical intracellular antioxidant more powerful than N-acetylcysteine and protects cellular components against oxidation, but pre-treatment with glutathione at 5 mM did not alter the shift (Fig. 3C). Dithiothreitol is a reducing agent and prevents formation of disulphide bridges between cysteine residues, which may cause a conformational change in E-cad, but pre-incubation with dithiothreitol at up to 10 mM did not affect the shift either (Fig. 3D). These results indicate that ROS are not involved in the mobility shift of E-cad *in vitro* under the conditions employed.

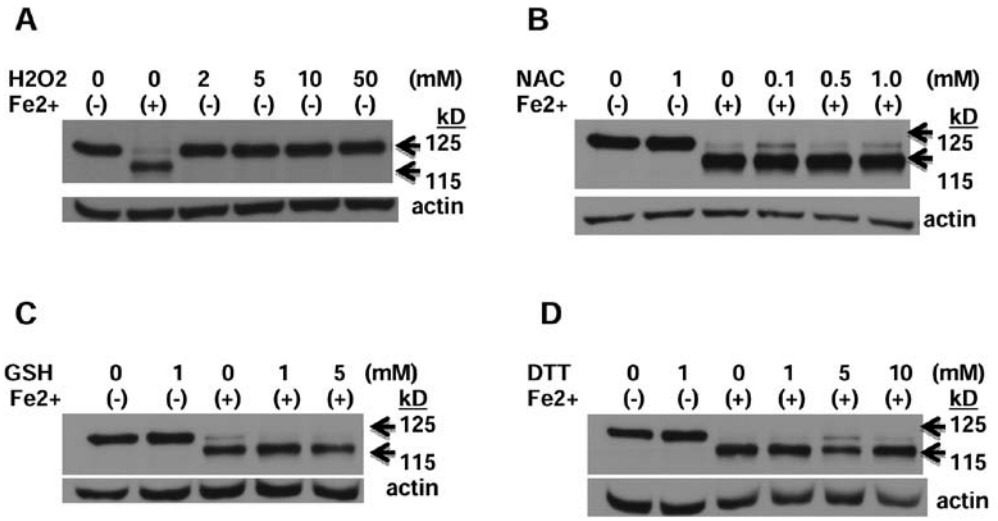

Fig. 3. Effect of oxidative stress on the mobility shift of E-cadherin *in vitro*. (**A**) Immunoblot of E-cad in control extracts treated with H_2O_2 (oxidant) at different concentrations for 30 min at 30 °C. (**B**) Control extracts were first treated with NAC (antioxidant) for 5 min at 30 °C and subsequently with $FeSO_4$ at 1mM for 30 min at 30 °C. (**C**) Control extracts were first treated with GSH (antioxidant) for 5 min at 30 °C and subsequently with $FeSO_4$ at 1 mM. (**D**) Control extracts were first treated with DTT (antioxidant) for 5 min at 30 °C and subsequently with $FeSO_4$ at 1 mM. Fe2+, $FeSO_4$.

Reversibility of the mobility shift

Deferoxamine is an iron chelator and is used in chelation therapy for iron removal in transfusional iron overload. DFO chelates iron by binding it in the blood; the resulting DFO-iron complex is excreted in urine and stool (Neufeld, 2006). Therefore, we tested DFO with the 115 kDa E-cad. The 115 kDa E-cad produced by the treatment of control extracts with $FeSO_4$ at 1 mM was shifted back to 125 kDa upon incubation with DFO at 2 mM (Figs. 4. 3, 5). Similarly, the 115 kDa E-cad from the iron-overloaded mice generated by injection of iron dextran was converted to 125 kDa by incubation with DFO at 1 mM (Figs. 4. 7, 8). These results clearly demonstrated that the mobility shift is reversible.

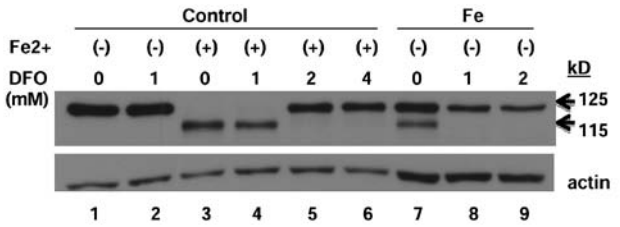

Fig. 4. Iron chelator reverses the mobility shift of E-cadherin *in vitro*. Immunoblot of E-cad in LB extracts treated with $FeSO_4$ and/or DFO. Control extracts were first treated with $FeSO_4$ at 1 mM for 30 min at 30 °C and subsequently with DFO at different concentrations for further 30 min. Fe samples were treated with DFO only. C, C57BL/6 control; Fe, C57BL/6 iron overload by injection of iron dextran; DFO, deferoxamine; Fe2+, $FeSO_4$.

Immunohistochemistry

In order to observe the effects of iron overload at the cellular level, the liver samples were analysed by immunohistochemistry. Iron deposition (blue) was detected only in the iron overload sample (Fig. 5A, B), clearly demonstrating a sign of iron overload at the cellular level. Whereas in the control sample E-cad (brown) was clearly detected at the plasma membrane around bile ducts and/or intrahepatic vessels, in the iron overload counterpart, weaker staining of the protein was observed (Fig. 5C, D), demonstrating that the effect of iron overload on the cellular expression of E-cad in the liver is evident and detectable at this stage of iron overload.

Discussion

Cadherins are membrane-bound proteins which associate, directly and indirectly, with numerous regulatory proteins at both cytoplasmic and extracellular domains, and thus cadherins are key components associated with many mechanisms that regulate the integrity of AJs (Zaidel-Bar, 2013). Since E-cad is the major cadherin in liver epithelial cells and its dysfunction is known to lead to tissue injury and eventually to carcinogenesis, we investigated E-cad in order to detect initial alteration(s) by iron overload in the liver, which may result in hepatocellular carcinoma. Our investigation of the liver from iron-overloaded mice revealed that iron overload causes an alteration of E-cad, which was detected as a mobility shift in SDS-PAGE under reducing conditions; the shift was found to be reversible, and the cellular expression of E-cad was decreased. The present study is the first to report a reversible mobility shift of E-cad.

The mobility shift of E-cad was demonstrated by immunoblotting of liver extracts from mice with disruption of the haemojuvelin gene, a mouse model of juvenile haemochromatosis (Niederkofler et al., 2005)

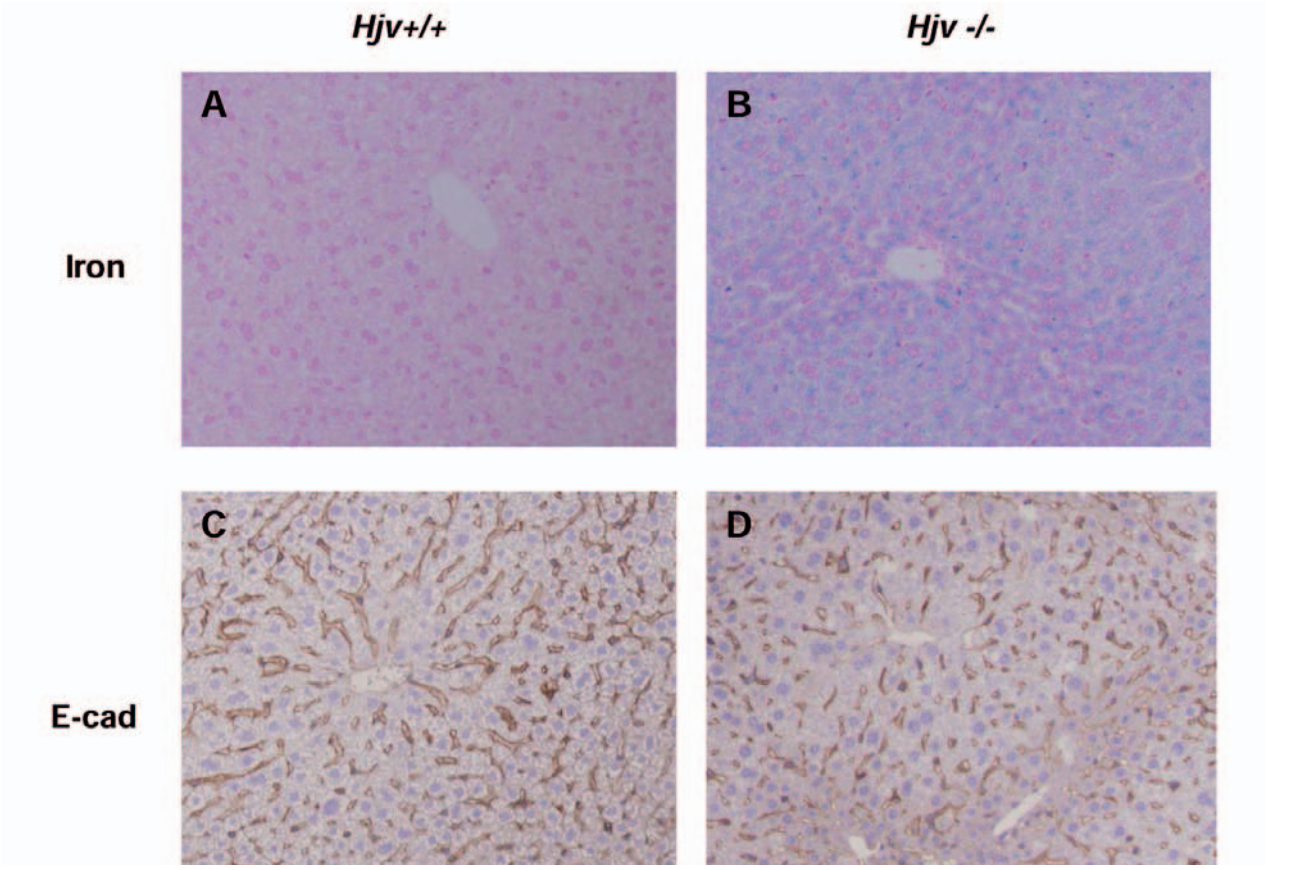

Fig. 5. Immunohistochemistry of E-cadherin in the liver. (**A**) $Hjv^{+/+}$, control, and (**B**) $Hjv^{-/-}$, iron overload by haemojuvelin gene disruption, a mouse model of juvenile hemochromatosis, were stained for iron (blue). (C) $Hjv^{+/+}$ and (D) $Hjv^{-/-}$ were stained for E-cad (brown). Original magnification, 400×.

previously studied in our laboratory (Krijt et al. 2012), and also from mice injected with iron dextran, a model of acquired iron overload. The detection of the shift in both samples confirmed an alteration by iron overload, which was not strain-specific. Fractionation revealed that a fraction of 115 kDa E-cad was endosome-bound. In the P3 endosomal fraction of the $Hjv^{-/-}$ sample, only the 115 kDa E-cad was detected with lower intensity, suggesting that the alteration is more pronounced in the endosomal fraction and that E-cad in the fraction is rather subjected to degradation than to recycling. The effects of iron on E-cad have not been previously fully elucidated. Bilello et al. (2003), using rat hepatocytes in long-term DMSO culture, reported that iron loading of hepatocytes resulted in decreased E-cad promoter activity and subsequently decreased E-cad mRNA and protein expression. In our study of the livers from iron-overloaded mice, decreased cellular expression of E-cad was observed in immunohistochemistry, but no significant change of the E-cad mRNA level was detected, suggesting that the mobility shift is posttranslational. The discrepancy of the observation may be due to different experimental conditions. It should be noticed that in order to detect initial alteration(s) of E-cad caused by iron overload, which might be minute, a buffer containing a mild detergent (0.5% NP-40) was used, by which E-cad affected by the increased level of iron is extracted but not E-cad in the stable AJs (Fukumoto et al., 2008). The majority of intact E-cad in the stable AJs, which would obscure detection of the alteration, i.e. the 115 kD E-cad, by its large quantity, was precipitated by low centrifugal force (Tsukita and Tsukita, 1989) and thus excluded from the analysis.

Iron overload could generate ROS, which inflict damage on cellular macromolecules such as lipids, proteins, and DNA. The association of iron overload with a high risk for carcinogenesis was previously reported (Huang, 2003), and Deugnier (2003) reported that the induction of oxidative stress caused by ROS is regarded to be a mechanism by which iron acts in carcinogenesis. Therefore, oxidative stress constitutes a plausible cause of the mobility shift. However, our study of oxidative stress did not indicate any effects of ROS on the mobility shift *in vitro*. It thus seems likely that ROS are not directly involved in the alteration that causes the mobility shift of E-cad.

Interestingly, the treatment with DFO to remove Fe^{2+} *in vitro* resulted in the reversal of the mobility shift. The observation provides an interesting new feature of the alteration of E-cad by iron overload. The reversal occurs not only for the 115 kDa E-cad generated by the treatment of control extract with Fe^{2+} *in vitro*, but also for that in the liver from iron-overloaded mice, indicating that the 115 kDa E-cad molecules from the two distinct

samples represent the same polypeptide. Thus, it may also imply that the alteration by iron overload *in vivo* is reversible. Also, the observation eliminates possible causes for the shift such as transcriptional control, proteolysis, and deglycosylation. The reversibility also confirms no participation of ROS in the shift. Therefore, it points toward a conformational change as a possible cause of the shift, and also possible direct involvement of Fe^{2+} in the change. Toxic metal cadmium was reported to disrupt cadherin function in the kidney by displacing Ca^{2+} from its binding sites at the extracellular domain, possibly causing a conformational change (Prozialeck et al., 2003). However, displacement of Ca^{2+} by Fe^{2+} in cadherin is not known. Meanwhile, it is known that the negatively charged phosphate group has high affinity to metal ions (Machida et al., 2007). Since E-cad is phosphorylated at the normal state and there are several potential phosphorylation sites at the C-terminus in the cytoplasmic domain (Stappert and Kemler, 1994), it is possible that an interaction between the Fe ion and phosphate groups takes place, which could result in a conformational change, and thus the mobility shift. Phosphorylation is known to cause the mobility shift of catenins due to a possible conformational change (Calautti et al., 1998; Fukumoto et al., 2008), and also to regulate the function of the cadherin/catenin complex (Zaidel-Bar, 2013), and therefore investigation of the phosphorylation sites in E-cad would be the next step to elucidating the mobility shift.

Immunohistochemistry detected decreased cellular expression of E-cad. Since the mobility shift is not caused by proteolysis, the antibody should equally detect both forms of E-cad, 115 and 125 kDa. The difference between the control and the iron overload sample in immunohistochemistry may therefore be due to that either some fraction of the 115 kDa E-cad is degraded, or the epitope is less accessible to the antibody in the 115 kDa E-cad, perhaps due to a conformational change, or both. The vulnerability of the 115 kD E-cad was detected in the P3 fraction. Interestingly, the epitope of the employed antibody is located near the potential multiple phosphorylation site at the C-terminus. Thus, the lower accessibility to the antibody cannot be excluded. The iron dose dependency of the mobility shift, *in vitro* as well as *in vivo*, and the decreased cellular expression detected by immunohistochemistry suggest that increasing amounts of iron would result in more pervasive alteration of E-cad, and thus more progressed cellular damage. Our observation fits well with the finding that the intensity of the cadherin signal gradually weakens from non-tumorous tissue to tumour regions in hepatocellular carcinomas (Zhai et al., 2008).

The mobility shift is caused by an alteration of E-cad induced by iron overload, which would result in weakened cell adhesions in AJs and could eventually lead to the onset of carcinogenesis. Further studies of the alteration may therefore provide a new insight into the roles of E-cad in AJs and also contribute to better understanding the pathology caused by iron overload, which could lead to the development of therapeutic methods.

Acknowledgement

The authors are grateful to Dr. Christine Bartels for critical reading of the manuscript.

References

Alves, C. C., Carneiro, F., Hoefler, H., Becker, K. F. (2009) Role of the epithelial-mesenchymal transition regulator Slug in primary human cancers. *Front. Biosci.* **14,** 3035-3050.

Berx, G., Becker, K. F., Hofler, H., van Roy, F. (1998) Mutations of the human E-cadherin (CDH1) gene. *Hum. Mutat*. **12,** 226-237.

Bilello, J. P., Cable, E. E., Isom, H. C. (2003) Expression of E-cadherin and other paracellular junction gene is decreased in iron-loaded hepatocytes. *Am. J. Pathol*. **162,** 1323-1338.

Calautti, E., Cabodi, S., Stein, P. L., Hatzfeld, M., Kedersha, N., Dotto, G. P. (1998) Tyrosine phosphorylation and Src family kinases control keratinocyte cell-cell adhesion. *J. Cell Biol*. **141,** 1449-1465.

Davis, M. A., Ireton, R. C., Reynolds, A. B. (2003) A core function for p120-catenin in cadherin turnover. *J. Cell Biol*. **163,** 525-534.

Deugnier, Y. (2003) Iron and liver cancer. *Alcohol* **30,** 145-150.

Fukumoto, Y., Shintani, Y., Reynolds, A. B., Johnson, K. R., Wheelock, M. J. (2008) The regulatory or phosphorylation domain of p120 catenin controls E-cadherin dynamics at the plasma membrane. *Exp. Cell Res.* **314,** 52-67.

Guarino, M., Tosoni, A., Nebuloni, M. (2009) Direct contribution of epithelium to organ fibrosis: epithelial-mesenchymal transition. *Hum. Pathol.* **40,** 1365-1376.

Halliwell, B., Gutteridge, J. M. C. (1990) The role of free radicals and catalytic metal ions in human diseases. *Methods Enzymol.* **186,** 1-85.

Hirohashi, S. (1998) Inactivation of the E-cadherin-mediated cell adhesion system in human cancers. *Am. J. Pathol.* **153,** 333-339.

Hoshino, T., Sakisaka, T., Baba, T., Yamada, T., Kimura, T., Takai, Y. (2005) Regulation of E-cadherin endocytosis by nectin through afadin, rap1, and $p120^{ctn}$. *J. Biol. Chem.* **280,** 24095-24103.

Huang, X. (2003) Iron overload and its association with cancer risk in humans: evidence for iron as a carcinogenic metal. *Mutat. Res*. **533,** 153-171.

Huber, A. H., Stewart, D. B., Laurents, D. V., Nelson, W. J., Weis, W. I. (2001) The cadherin cytoplasmic domain is unstructured in the absence of β-catenin. *J. Biol. Chem*. **276,** 12301-12309.

Krijt, J., Frýdlová, J., Kukačková, L., Fujikura, Y., Přikryl, P., Vokurka, M., Nečas, E. (2012) Effect of iron overload and iron deficiency on liver hemojuvelin protein. *PLoS One* **7,** e37391.

Le, T. L., Yap, A. S., Stow, J. L. (1999) Recycling of E-cadherin: a potential mechanism for regulating cadherin dynamics. *J. Cell Biol.* **146,** 219-232.

Machida, M., Kosako, H., Shirakabe, K., Kobayashi, M., Ushiyama, M., Inagawa, J., Hirano, J., Nakano, T., Bando, Y.,

Nishida, E., Hattori, S. (2007) Purification of phosphoproteins by immobilized metal affinity chromatography and its application to phosphoproteome analysis. *FEBS J.* **274,** 1576-1587.

Meng, W., Takeichi, M. (2009). Adherens junction: molecular architecture and regulation. *Cold Spring Harb. Perspect. Biol.* **1,** a002899.

Miyashita, Y., M. Ozawa. (2007) Increased internalization of p120-uncoupled E-cadherin and a requirement for a dileucine motif in the cytoplasmic domain for endocytosis of the protein. *J. Biol. Chem.* **282,** 11540-11548.

Nanes, B. A., Chiasson-MacKenzie, C., Lowery, A. M., Ishiyama, N., Faundez, V., Ikura, M., Vincent, P. A., Kowalczyk, A. P. (2012) p120-catenin binding masks an endocytic signal conserved in classical cadherins. *J. Cell Biol.* 199, 365-380.

Neufeld, E. J. (2006) Oral chelators deferasirox and deferiprone for transfusional iron overload in thalassemia major: new data, new questions. *Blood* **107,** 3436-3441.

Niederkofler, V., Salie, R., Arber, S. (2005) Hemojuvelin is essential for dietary iron sensing, and its mutation leads to severe iron overload. *J. Clin. Invest*. **115,** 2180-2186.

Papanikolaou, G., Pantopoulos, K. (2005) Iron metabolism and toxicity. *Toxicol. Appl. Pharmacol.* **202,** 199-211.

Pietrangelo, A. (2003) Haemochromatosis. *Gut* **52,** 23-30.

Pinho, S. S., Seruca, R., Gärtner, F., Yamaguchi, Y., Gu, J., Taniguch, N., Reis, C. A. (2011) Modulation of E-cadherin function and dysfunction by N-glycosylation. *Cell Mol. Life Sci.* **68,** 1011-1020.

Ponka, P., Beaumont, C., Richardson, D. R. (1998) Function and regulation of transferrin and ferritin. *Semin. Hematol.* **35,** 35-54.

Prozialeck, W. C., Lamar, P. C., Lynch, S. M. (2003) Cadmium alters the localization of N-cadherin, E-cadherin, and β-catenin in the proximal tubule epithelium. *Toxicol. Appl. Pharmacol*. **189,** 180-195.

Reynolds, A. B., Daniel, J., McCrea, P. D., Wheelock, M. J., Wu, J., Zhang, Z. (1994) Identification of a new catenin: the tyrosine kinase substrate p120cas associates with E-cadherin complexes. *Mol. Cell Biol.* **14,** 8333-8342.

Sebastiani, G., Pantopoulos, K. (2011) Disorders associated with systemic or local iron overload: from pathophysiology to clinical practice. *Metallomics* **3,** 971-986.

Stappert, J., Kemler, R. (1994) A short core region of E-cadherin is essential for catenin binding and is highly phosphorylated. *Cell Adhes. Commun.* **2,** 319-327.

Taguchi, K., Ishiuchi, T., Takeichi, M. (2011) Mechanosensitive EPLIN-dependent remodeling of adherens junctions regulates epithelial reshaping. *J. Cell Biol*. **194,** 643-656.

Tsukita, S., Tsukita, S. (1989) Isolation of cell-to-cell adherens junctions from rat liver. *J. Cell Biol*. **108,** 31-41.

Xiao, K., Allison, D. F., Buckley, K. M., Kottke, M. D., Vincent, P. A., Faundez, V., Kowalczyk, A. P. (2003) Cellular levels of p120 catenin function as a set point for cadherin expression levels in microvascular endothelial cells. *J. Cell Biol*. **163,** 535-545.

Zaidel-Bar, R. (2013) Cadherin adhesome at a glance. *J. Cell Sci.* **126,** 373-378.

Zhai, B., Yan, H. X., Liu, S. Q., Chen, L, Wu, M. C., Wang, H. Y. (2008) Reduced expression of E-cadherin/catenin complex in hepatocellular carcinomas. *World J. Gastroenterol*. **14,** 5665-5673.